PCCP

Elucidating the Chemical Dynamics of the Elementary Reactions of the 1-Propynyl Radical (CH_3CC; X^2A_1) with 2-Methylpropene ($(CH_3)_2CCH_2$; X^1A_1)

Journal:	*Physical Chemistry Chemical Physics*
Manuscript ID	CP-ART-12-2023-005872.R1
Article Type:	Paper
Date Submitted by the Author:	11-Jan-2024
Complete List of Authors:	Medvedkov, Iakov ; University of Hawai'i at Manoa, Chemistry Nikolayev, Anatoliy; Samara National Research University S P Korolev Yang, Zhenghai; University of Hawai'i at Manoa, Chemistry Goettl, Shane; University of Hawai'i at Manoa Mebel, Alexander; Florida International University, Chemistry and Biochemistry Kaiser, Ralf; University of Hawai'i at Manoa

ARTICLE

Elucidating the Chemical Dynamics of the Elementary Reactions of the 1-Propynyl Radical (CH_3CC; X^2A_1) with 2-Methylpropene ($(CH_3)_2CCH_2$; X^1A_1)

Received 00th January 20xx,
Accepted 00th January 20xx

DOI: 10.1039/x0xx00000x

Iakov A. Medvedkov,[a] Anatoliy A. Nikolayev,[b] Zhenghai Yang,[a] Shane J. Goettl,[a] Alexander M. Mebel,[c*] and Ralf I. Kaiser[a*]

Exploiting the crossed molecular beam technique, we studied the reaction of the 1-propynyl radical (CH_3CC; X^2A_1) with 2-methylpropene (isobutylene; $(CH_3)_2CCH_2$; X^1A_1) at a collision energy of 38 ± 3 kJ mol^{-1}. The experimental results along with *ab initio* and statistical calculations revealed that the reaction has no entrance barrier and proceeds via indirect scattering dynamics involving C_7H_{11} intermediates with lifetimes longer than their rotation period(s). The reaction is initiated by the addition of the 1-propynyl radical with its radical center to the π-electron density at the C1 and/or C2 position in 2-methylpropene, which can isomerize to each other. Further, the C_7H_{11} intermediate formed from the C1 addition either emits atomic hydrogen or undergoes isomerization via [1,2-H] shift from the CH_3 or CH_2 group prior to atomic hydrogen loss preferentially leading to 1,2,4-trimethylvinylacetylene (2-methylhex-2-en-4-yne) as the dominant product. The molecular structures of the collisional complexes promote hydrogen atom loss channels. RRKM results show that hydrogen elimination channels dominate in this reaction, with a branching ratio exceeding 70 %. Since the reaction of the 1-propynyl radical with 2-methylpropene has no entrance barrier, is exoergic, and all transition states involved are located below the energy of the separated reactants, bimolecular collisions are feasible to form trimethylsubstituted 1,3-enyne (**p1**) via a single collision event even at temperatures as low as 10 K prevailing in cold molecular clouds such as G+0.693. The formation of trimethylsubstituted vinylacetylene could serve as the starting point of fundamental molecular mass growth processes leading to di- and trimethylsubstituted naphthalenes via the HAVA mechanism.

Introduction

The interstellar medium (ISM) is known to be a well-stocked source of hydrocarbons[1] (Fig. 1). These hydrocarbons along with their (resonantly stabilized) radicals have been suggested to act as precursors to polycyclic aromatic hydrocarbons (PAHs). Along with their derivates, i.e. protonated, ionized, (de)hydrogenated, alkylated, and nitrogen-substituted counterparts, PAHs are believed to account for up to 30 % of the cosmic carbon budget.[2–8] The PAHs (derivatives) have been also postulated as carriers of the unidentified infrared emission (UIE) bands observed in the range of 3–14 μm[9] with prominent UIE features such as 3.3, 6.2, 7.7, 8.6, and 11.3 μm closely resembling with the characteristic vibrational frequencies of aromatic C–C and C–H bonds. However, only recently one- and two-ringed aromatic molecules such as benzene (C_6H_6),[10] indene (C_9H_8),[11,12] benzonitrile (C_6H_5CN),[13] 2-cyanoindene (2-C_9H_7CN),[14] ethynylbenzene (C_6H_5CCH),[15] benzyne (C_6H_4),[16] and cyanonaphthalenes ($C_{10}H_7CN$)[17] were detected in the cold molecular cloud TMC-1 with the origin of PAHs in deep space still a topic of the intense debate. The detection of benzene in the carbon-rich protoplanetary nebula CRL 618[10] may suggest a bottom-up synthesis of aromatic structures via small hydrocarbons.[18] One prominent route emerged recently in the form of the barrierless **H**ydrogen **A**bstraction **V**inylacetylene **A**ddition (HAVA) mechanism.[2,19–24] This mechanism commences with a barrierless formation of a van-der-Waals complex in the reaction of vinylacetylene (CH_2CHCCH) and an aryl radical such as phenyl (C_6H_5) followed by isomerization of the latter via addition with the transition state residing lower than the energy of the separated reactants (submerged barrier). This addition leads to a resonantly stabilized free radical (RSFR) intermediate which eventually undergoes ring closure, hydrogen shift, and aromatization via an atomic hydrogen loss. Also, the replacement of phenyl[23] or vinylacetylene by methyl-substituted reactants[25] resulted in the methyl-substituted PAHs, whose formation is even less understood; these molecules are believed [26–30] to be responsible for the 3.4 μm feature of the UIE.[31–33]

Obviously, an *in situ* formation of PAHs in deep space must involve hydrocarbon molecules present in cold molecular

[a] Department of Chemistry, University of Hawai'i at Manoa, Honolulu, HI 96822, USA
[b] *Samara National Research University, Samara 443086, Russia*
[c] *Department of Chemistry and Biochemistry, Florida International University, Miami, Florida 33199, USA*
Corresponding to: ralfk@hawaii.edu; mebela@fiu.edu

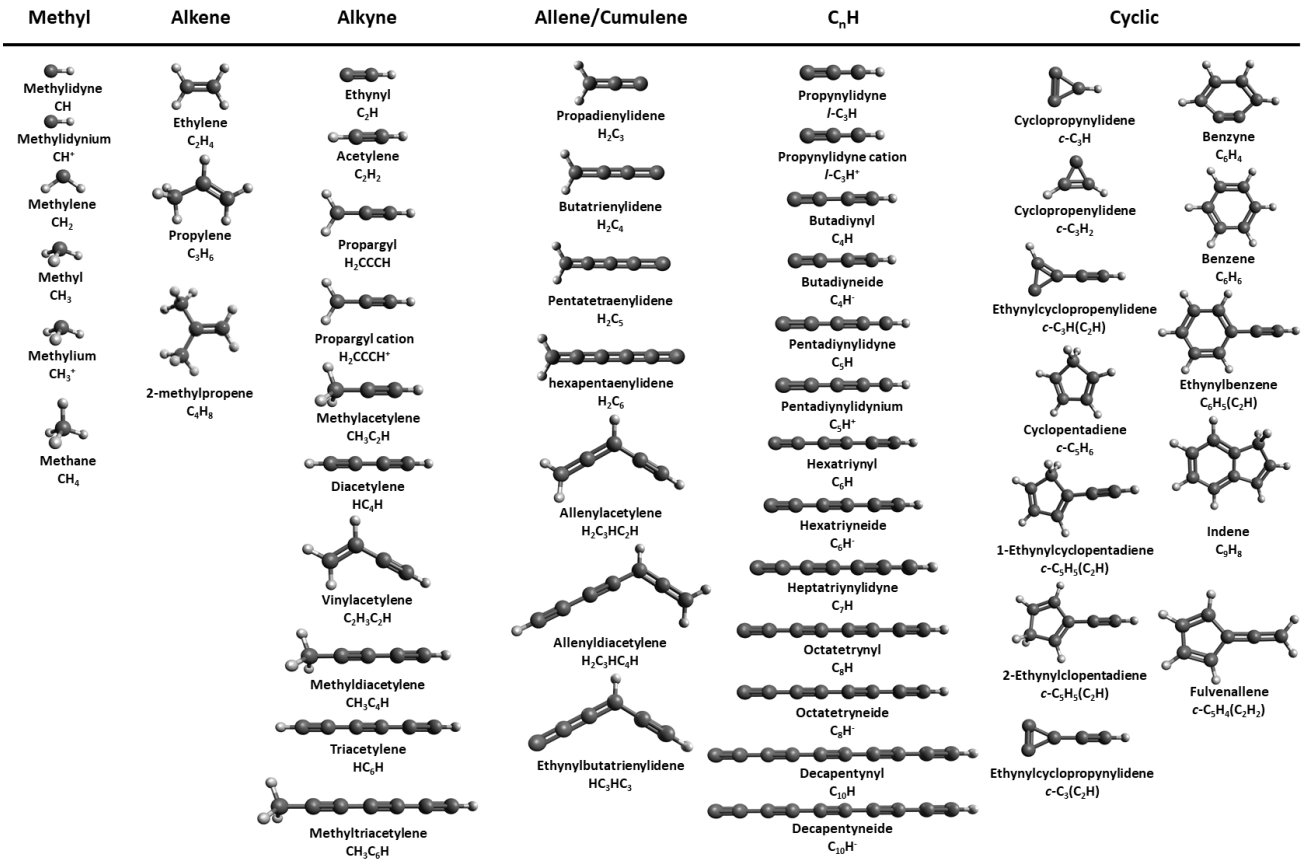

Figure 1. Hydrocarbon molecules detected in deep space to date.

clouds. A systematic investigation of reactions leading to aromatics represents an indispensable step toward understanding the chemistry of PAHs in cold molecular clouds. The recent detection of 2-methylpropene (isobutylene; C_4H_8; $(CH_3)_2CCH_2$) [34] in the molecular cloud G+0.693 brings up questions about its chemistry and its role in the chemical evolution of cold clouds. While the mutual chemistry of CH_x (x=0, 1), C_2H_x (x =0 – 4), C_3H_x (x=0, 3, 4, 6) C_4H_x (x=2, 4, 6), and C_6H_x (x=5, 6) under conditions relevant to cold molecular clouds has been well studied both experimentally and theoretically,[24,35–42] the chemical reactions of C_4H_8 under single collision conditions have been largely elusive. The reaction of C_4H_8 isomers with the ethynyl (C_2H) radical was studied experimentally at 79 K exploiting the CRESU (Cinétique de Réaction en Ecoulement Supersonique Uniforme, or Reaction Kinetics in Uniform Supersonic Flow) technique;[43] this system has also been explored theoretically[44] with *ab initio* calculations (B3LYP/6-31 + G**) augmented with statistical calculations. The 1-propynyl radical (CH_3CC) – a non-resonance high energy isomer of the resonantly stabilized propargyl radical (H_2CCCH) – has received considerable attention for its role in molecular mass growth processes in carbon-rich extraterrestrial environments due to its barrierless addition to carbon-carbon double and triple bonds of hydrocarbons even at low temperatures.[25,45–52] Although 1-propynyl has not yet been detected in extraterrestrial environments, TMC-1[53,54] and G+0.693[55] exhibit high fractional abundances of its potential precursor propyne (methylacetylene; CH_3CCH). Recently,[25] our group explored the reaction of the 1-propynyl radical with propene (CH_3CHCH_2); this elementary reaction leads to 1,3-dimethylvinylacetylene (2-hexen-4-yne) highlighting the role of methyl- and dimethyl-substituted vinylacetylenes in the formation of alkylated PAHs via the aforementioned HAVA mechanism. Therefore, the reaction of the 1-propynyl radical with the recently observed interstellar 2-methylpropene deserves to be studied as a possible formation pathway for trimethyl substituted vinylacetylenes. In addition, while in astrochemistry, molecules carrying a conjugated double and triple bond (Fig. 2) are referred to as 'vinylacetylenes', in synthetic organic chemistry this moiety is labelled as a '1,3-enyne' structure. In preparative organic chemistry, substituted 1,3-enynes are widely exploited in bioactive molecules,[56] functional materials,[57,58] and complexity-building

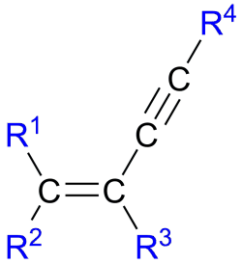

Figure 2. Molecular structure of substituted 1,3-enynes (vinylacetylenes).

transformations,[59] in the synthesis of furan[60] and pyridine.[61,62–64] In addition, the enyne motif is present in both natural and artificial biologically active compounds such as dopamine agonists.[65]

In this article, we present an experimental and theoretical investigation of the formation of 1,2,4-trimethylvinylacetylene (2-methylhex-2-en-4-yne) under single collision conditions through the elementary gas phase reaction of the 1-propynyl radical (CH_3CC; X^2A_1) with 2-methylpropene ($(CH_3)_2CCH_2$; X^1A') exploiting crossed molecular beams. We also exploit the HAVA mechanism to predict the role of 1,2,4-trimethylvinylacetylene – and of substituted 1,3-enynes in general – in the formation of distinct di- and tri-substituted naphthalene isomers in deep space to provide new knowledge toward the understanding of how alkylated PAHs may form in deep space.

Experimental and Computational

Experimental

The gas-phase reaction of the 1-propynyl radical (CH_3CC; X^2A_1) with 2-methylpropene (isobutene; $(CH_3)_2CCH_2$; X^1A_1) was carried out under single-collision conditions using the crossed molecular beams machine.[66,67] The experimental setup, data acquisition, and data processing have been discussed previously;[45,46,49] here we will only provide a brief description. A pulsed (60 Hz) supersonic beam of the 1-propynyl radical was prepared by photodissociation of 1-iodopropyne (CH_3CCI; TCI, 99%+) seeded at a level of 0.5% in helium (He, 99.9999 %, Matheson) at a backing pressure of 760 Torr using the 193 nm output of the excimer laser (Coherent, CompEx110; 20 mJ pulse^{-1}; 30 Hz) focused (2 × 6 mm^2) at the exit of the primary pulsed valve 2 mm downstream.[45,46,49] The molecular beam was skimmed and velocity selected using a four-slot chopper wheel; this achieved a peak velocity v_p = 1660 ± 49 m s^{-1} and speed ratio S = 9 ± 2. The secondary molecular beam (60 Hz, v_p = 756 ± 29 m s^{-1}, S = 7 ± 1) of neat 2-methylpropene (550 Torr; $(CH_3)_2CCH_2$; Sigma-Aldrich, 99%) was pulsed 90 μs prior to the primary beam. Both molecular beams intersected at an angle of 90° in the scattering chamber at a mean collision energy of E_C = 38 ± 3 kJ mol^{-1}. The reactively scattered products were ionized by electron ionization at 80eV (2mA) at the entrance of the rotatable detector, filtered according to mass-to-charge ratios (m/z) by the QMS (Extrel, QC 150; 2.1 MHz), and detected using a Daly-type particle ion counter.[68] The detector is rotatable in the scattering plane defined by the primary and secondary beams. Angularly resolved time-of-flight (TOF) spectra were recorded at discrete laboratory angles in 2.5° steps. Operating laser at 30 Hz and the pulsed valve at 60 Hz allowed a background subtraction ("laser-on" minus "laser-off") during the TOF recording. We should note that the formation of the propargyl radical (2-propynyl, H_2CCCH) is possible in the photolysis zone via isomerization of the 1-propynyl radical through sequential hydrogen shifts. At the same time, the entrance barrier for the addition of the propargyl radical to the C=C double bond is 51–59 kJ mol^{-1}, which is well above the collision energy in our experiments (38 ± 3 kJ mol^{-1}). Therefore, even if propargyl is present in the molecular beam as the result of isomerization from 1-propynyl, the propargyl radical cannot contribute to the reactive scattering signal.

To gain information on the reaction dynamics, TOF spectra and the laboratory angular distribution (LAD) were fitted with the forward-convolution technique.[69,70] This approach uses initially a trial angular flux $T(\theta)$ and translational energy $P(E_T)$ distributions in the center-of-mass (CM) frame to simulate the laboratory data (TOFs and LAD). CM functions were then iteratively varied until the best fit of the TOF spectra and LAD were achieved. Together the CM functions represent the reactive differential cross section $I(\theta, u)$ the CM velocity u, $I(u, \theta) \sim P(u) \times T(\theta)$, which is represented as a flux contour map (Fig. 4c) thus depicting an overall image of the reaction outcome.

Computational

Geometry optimization of numerous stationary structures such as reactants, intermediates, transition states, and products located on the C_7H_{11} potential energy surface (PES) of the 1-propynyl plus 2-methylpropene reaction was carried out at the long-range corrected hybrid density functional (DFT) ωB97X-D level of theory[71] in combination with Pople's split-valence 6-311G(d,p) basis set. The same conjunction was applied to calculate vibrational frequencies for each optimized molecular structure. The later computations have made it possible to evaluate zero-point vibrational energy corrections (ZPE) and subsequently to obtain unimolecular rate constants and branching ratios. To increase the accuracy of the DFT relative energies of all the species which do not comply with the required chemical accuracy to reasonably compare theoretical and experimental results, the explicitly correlated coupled cluster CCSD(T)-F12 approach[72,73] with the variational method for single and double excitations and the perturbation theory for triple excitations accompanied by Dunning's correlation-consistent cc-pVTZ-f12 basis set[74] was used for single-point energy calculations at the optimized geometries. The aggregate CCSD(T)-F12/cc-pVTZ-f12//ωB97X-D/6-311G(d,p) + ZPE[ωB97X-D/6-311G(d,p)] theoretical scheme is projected to provide the accuracy within 4 kJ mol^{-1} or even better.[75] The electronic structure calculations were carried out by means of the GAUSSIAN 09[76] and MOLPRO 2015[77] quantum chemistry software packages.

Energy-dependent rate constants of all unimolecular reaction steps taking place on the C_7H_{11} PES after the primary bimolecular association stage were obtained utilizing the Rice-Ramsperger-Kassel-Marcus (RRKM) method[78] at the zero-pressure limit to simulate the crossed molecular beam single collision conditions that emulate an outer space environment. The internal energy for all the C_7H_{11} isomers was set to be equal to the sum of the collision and chemical activation energies. The latter term is derived as a negative of the relative energy for all compounds with respect to the separated 1-propynyl plus 2-methylpropene reactants. The RRKM calculations were performed by using our in-house code Unimol.[47] Finally, the product branching ratios were evaluated in steady-state approximation using the calculated rate constants.

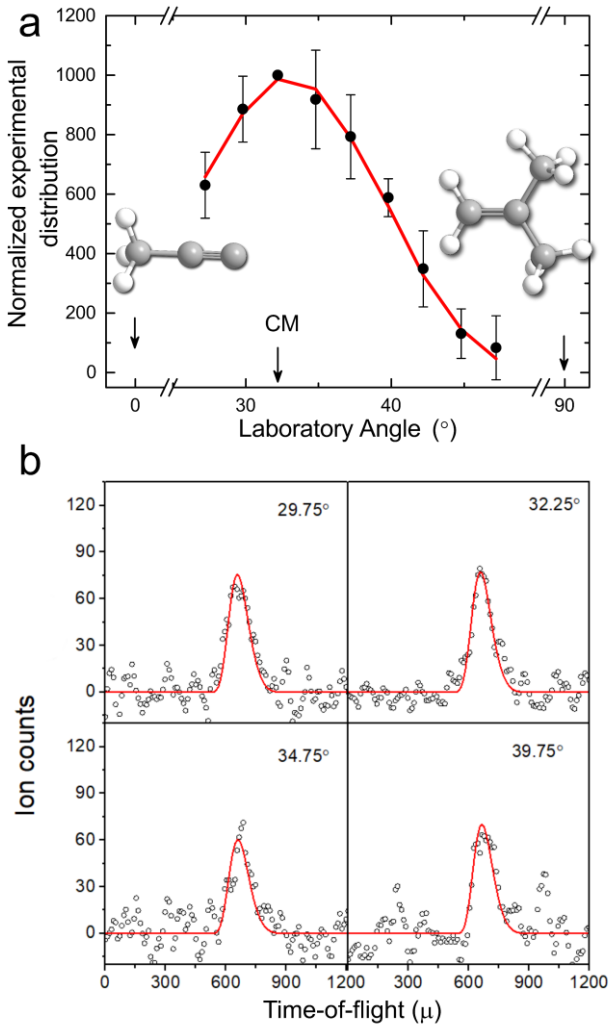

Figure 3. (a) Laboratory angular distribution (b) and time-of-flight (TOF) spectra recorded at m/z = 93 for the reaction of the 1-propynyl radical with 2-methylpropene at a collision energy of 38 ± 3 kJ mol^{-1}. The circles represent the experimental data and the solid lines the best fits.

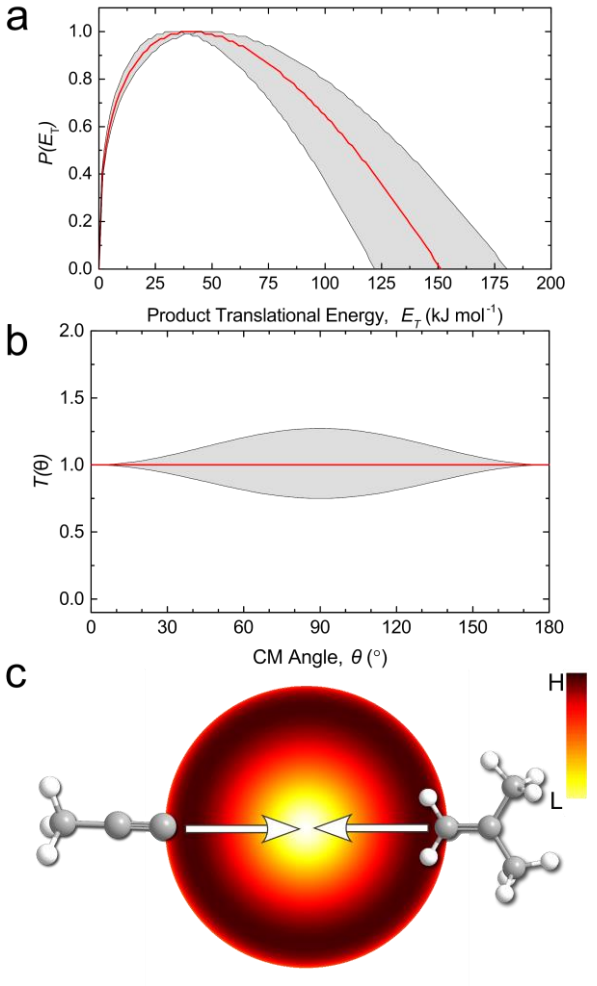

Figure 4. (a) Center-of-mass translational energy P(E_T), (b) angular T(θ) flux distributions, and (c) flux contour map for the reaction of the 1-propynyl radical with 2-methylpropene. The solid lines represent the best fit, while the shaded areas indicate the error limits. For T(θ), the direction of the 1-propynyl beam is defined as 0° and of the 2-methylpropene as 180°.

Results

Laboratory frame

The reactive scattering signal for the reaction of the 1-propynyl radical (CH_3CC; 39 amu) with 2-methylpropene ($(CH_3)_2CCH_2$; 56 amu) was observed at mass-to-charge ratios *m/z* = 94 ($C_7H_{10}^+$) and 93 ($C_7H_9^+$). The TOF spectra obtained at these two *m/z* overlap after scaling, suggesting that both m/z originate from the same reaction channel forming the C_7H_{10} product and atomic hydrogen (reaction (1)). Signal at *m/z* = 93, therefore, arises from dissociative electron impact ionization of the C_7H_{10} product in the electron impact ionizer. The presence of the background interference at *m/z* = 80, 79, and 78 prevented detection of a potential methyl loss channel (reaction (2)). Probable sources of the background signal are discussed in ESI.

CH_3CC (39 amu) + $(CH_3)_2C{=}CH_2$ (56 amu) → C_7H_{10} (94 amu) + H (1 amu) (1)

CH_3CC (39 amu) + $(CH_3)_2C{=}CH_2$ (56 amu) → C_6H_8 (80 amu) + CH_3 (15 amu) (2)

The best signal-to-noise ratio was detected at *m/z* = 93; hence, *m/z* = 93 was used to collect TOF spectra at discrete intervals in steps of 2.5° from 27.25° to 47.25° Θ (Fig. 3a). The resulting TOFs were then normalized with respect to the CM angle to obtain the laboratory angular distribution (Fig. 3b). Notable features of the LAD include its width of at least 20° and symmetry around the CM angle at 32.6 ± 0.4°. These findings propose that the C_7H_{10} products were formed via indirect scattering dynamics through complex formation involving one or more C_7H_{11} intermediates. [35,40,66].

Center-of-Mass Frame

The laboratory data could be fit with a single channel (reaction 1) with an energy-dependent reaction cross section proportional to $E_C^{-(2/3)}$ for entrance-barrierless reactions (Fig. 3a) dominated by long-range dipole–dipole interactions.[79] The best-fit CM functions are depicted in Fig. 4 where the grey-filled areas define the limits of the acceptable fits. Considering the translational energy flux distribution P(E_T) (Fig. 4a), the

maximum energy (E_{max}) represents the kinetic energy of those molecules born without internal excitation. The energy conservation dictates that $E_{max} = E_C - \Delta_r G$, where E_C and $\Delta_r G$ represent the collision energy and the reaction energy, respectively. The derived $P(E_T)$ terminates at 150 ± 29 kJ mol^{-1}. Subtracting from the collision energy of 38 ± 3 kJ mol $^{-1}$ gives us $\Delta_r G$ = –112 ± 32 kJ mol^{-1} for the atomic hydrogen loss channel (reaction (1)). Further, the distribution maximum of the $P(E_T)$ from 36 to 45 kJ mol^{-1} indicates a tight exit transition state in the exit channel and hence a significant electron reorganization from the decomposing C_7H_{11} complex(es) to the final products. The average translation energy of 57 ± 11 kJ mol^{-1} suggests that 38 % of the total energy is channeled into product translation, which further implies the formation of a covalently bound intermediate. Additional information on the reaction dynamics can be obtained from the CM angular distribution T(θ) (Fig. 4b). The 'flat' T(θ) reveals that products after a collision are scattered in all directions with equal probability (isotropic scattering). The forward-backward symmetry and intensity at all angles also propose indirect scattering dynamics through the C_7H_{11} complex(es) and lifetime(s) of C_7H_{11} intermediates longer than the(ir) rotational period(s).[79] These findings are also supported by the flux contour map (Fig. 4c), which shows an overall image of the reaction and the scattering process.

Discussion

Now we combine our experimental results with electronic structure and statistical calculations to uncover the underlying reaction mechanism and to infer the nature of formed C_7H_{10} isomers. The full potential energy surfaces (PES) (Fig. S1–S5) along with results of RRKM calculations (Table S1–S2) are compiled in the Supporting Information. These computational results are correlated with our experimental findings. There are twenty-four theoretically possible products (**p1**-**p4**, **p7**-**p25**) and eighteen (**i1**-**i6**, **i9**-**i20**) intermediates. The overall barrierless and exoergic reaction of 1-propynyl with 2-methylpropane involves indirect reaction dynamics and opens channels to three acyclic molecules (**p1-p3,** Fig. 5) via atomic hydrogen and methyl elimination processes through the six possible intermediates (**i1-i6**) connected by eight transition states. The calculations reveal that the reaction starts with an addition of the 1-propynyl radical without an entrance barrier to either the two chemically nonequivalent carbon atoms C1 or C2 of the olefinic carbon-carbon double bond of 2-methylpropane with its radical center (Fig. 5). This leads to the radical intermediates **i1** and/or **i4**. Stabilized by 225 and 238 kJmol^{-1} with respect to the separated reactants. Both intermediates can be interconverted via **i2** and **i3**, which formally represent derivatives of cyclopropane, through low-lying transition states. Alternatively, **i1** can undergo unimolecular decomposition via the loss of a methyl radical to form **p3**. The emission of the methyl radical involves a barrier almost twice as high (123 kJ mol^{-1}) compared to isomerization of **i1** to **i4** (64 kJ mol^{-1}); hence, the latter pathway should be favorable. Intermediate **i4** can undergo atomic hydrogen loss, yielding **p1** and/or **p2** in overall exoergic reactions. Alternatively, **i4** isomerizes via two distinct [1,2-H] shifts: (1) from the CH_3 group of C_4H_8 moiety to **i5** or (2) from the CH_2 group at the C1-position to form **i6**. Two radical intermediates **i5** and **i6** are connected by hydrogen loss channels to **p2** and **p1**, respectively.

Which product(s) dominate(s)? RRKM calculations (Table S1) predict that the atomic hydrogen loss channel is prevalent (>70%), while the methyl elimination only contributes to about 20%. The most likely product is the conjugated 1,3-enyne **p1** (2-methylhex-2-en-4-yne) with an overall yield of more than 60%, while **p2** (2-methylhex-1-en-4-yne) holds lower fractions of about 10%. The experimentally derived reaction energy of –112 ± 32 kJ mol^{-1} for the hydrogen atom loss elimination channels supports the formation of **p1** and/or **p2** (–119 and 96 kJ mol^{-1}) under our experimental conditions. Which actual pathways are prevalent in the reaction mechanism? The initially formed radical intermediates **i1** and **i4** tend to restore a closed shell molecule in the β-scission processes and form a conjugated system between a carbon-carbon double and triple bond, i.e. a vinylacetylene structural moiety. In general, carbon-carbon single bond cleavage and hence methyl loss to **p3** should be

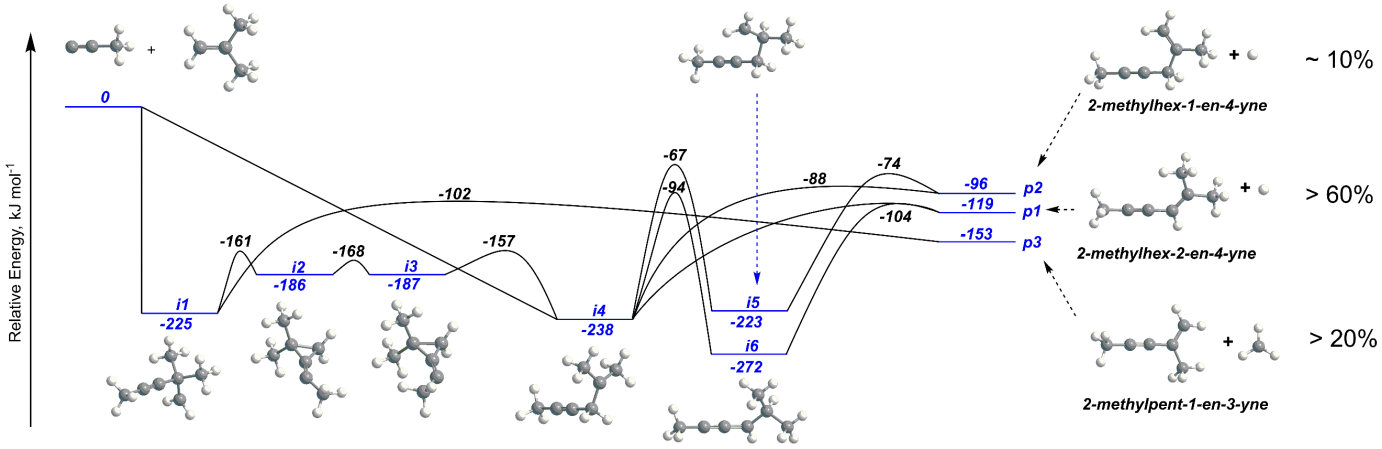

Figure 5. Potential energy surface for the bimolecular reaction of the 1-propynyl radical (CH_3CC; X^2A_1) with 2-methylpropene ($(CH_3)_2CCH_2$; X^1A') leading to C_7H_{10} + H and C_6H_8 + CH_3 products calculated at the CCSD(T)-F12/cc-pVTZ-F12//ωB97X-D/6-311G(d,p) level of theory. Relative energies are given in kJ mol^{-1} with respect to the reactants. Product branching ratios obtained from the RRKM calculations (Table S1) are shown on the right.

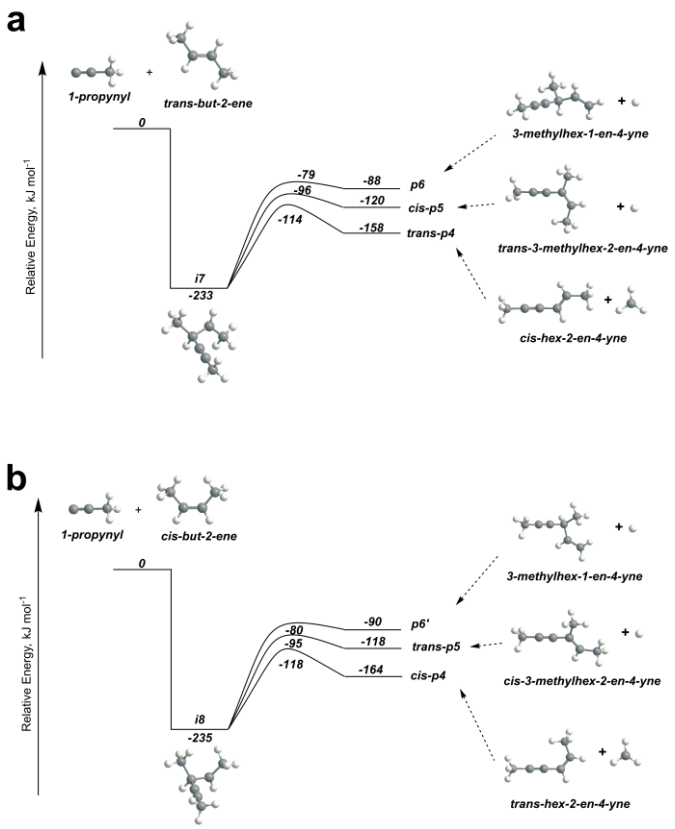

Figure 6. Potential energy surfaces for the bimolecular reactions of the 1-propynyl radical (CH_3CC; X^2A_1) with the *trans*- (a) and *cis*- (b) isomers of 2-butene ($CH_3CHCHCH_3$; X^1A'), considering only the addition-elimination mechanism, calculated at the CCSD(T)-F12/cc-pVTZ-F12//ωB97X-D/6-311G(d,p) level of theory. Relative energies are given in kJ mol^{-1} with respect to the reactants.

thermodynamically favorable and hence the methyl elimination channel should dominate. However, the presence of two methyl groups induces a steric hindrance attack and hence decreases the cone of acceptance [79] for a C2-attack to **i1**; in combination with the lack of steric hindrance of an addition to the CH_2 moiety, **i4** is the most probable initial complex. In addition, as discussed above, even if **i1** is formed, this collision complex undergoes facile isomerization to **i4** rather than methyl loss considering the unfavorable energy of the transition state of the latter pathway. Overall, **i4** preferentially undergoes hydrogen loss (95 %) rather than hydrogen shifts (5 %) eventually leading to **p1** and **p2**, respectively.

It should be noted that under the same experimental conditions, we also attempted the reaction of 1-propynyl radical (C_3H_3; X^2A_1) with *cis*-2-butene ($CH_3CHCHCH_3$; X^1A_1). No signal was detected at m/z = 94 and 93 in potential atomic and molecular hydrogen losses, while detection of the CH_3-loss channel was prevented by a high background signal at m/z = 80, 79, and 78. In order to rationalize this result, we conducted additional electronic structure and statistical calculations (Fig. 6, Table S3, S4) for a simple one step addition-elimination process in reactions of 1-propynyl with *cis*- and *trans*-2-butene. Here, both carbon atoms of the olefinic carbon-carbon double bond are chemically equivalent and hence only one initial reaction intermediate can be formed upon the reaction with *cis*-2- and *trans*-2-butene. This mechanism initiates with an addition of the 1-propynyl radical to C=C double bond in *trans*- and *cis*-2-butene forming **i7** (Fig. 6a) and **i8** (Fig. 6b) and follows competitive atomic hydrogen and methyl group loss channels from the collision complex to **p4** – **p6**. Results of the RRKM calculations reveal that the CH_3-loss channels forming ***trans*-** and ***cis*-p4** are the most probable decomposition pathways, exceeding 90% in the reactions with both 2-butene isomers. This reflects the experimental findings and the lack of observation of the atomic hydrogen loss pathway. This finding is the direct consequence of the lower barrier of decomposition of the initial reaction intermediates (117 to 119 kJ mol^{-1}) which is energetically favorable by 18 – 38 kJ mol^{-1} compared to the competing hydrogen loss pathways.

These findings are in line with previous investigations of chemically related systems. Statistical calculations of the 1-propynyl (CH_3CC) plus propene (C_3H_6) system revealed a dominant methyl loss channel (61±15%).[25] A combined experimental and computational study of the reaction of the ethynyl radical (C_2H) with 2-butene (C_4H_8) predicted a 100% methyl loss. These findings support our conclusion of reaction dynamics of substituted ethylenes driven by regio- and stereoselectivity due to the enhanced cone-of-acceptance of the least substituted olefinic carbon atom to which the doublet radical reactant adds and the lower barrier of a methyl loss compared to atomic hydrogen elimination.

Conclusions

Exploiting the crossed molecular beam technique, we studied the reaction of the 1-propynyl radical (CH_3CC; X^2A_1) with 2-methylpropene (isobutylene; $(CH_3)_2CCH_2$; X^1A_1) at a collision energy of 38 ± 3 kJ mol^{-1}. Experimental data were augmented by electronic structure (CCSD(T)-F12/cc-pVTZ-F12//ωB97X-D/6-311G(d,p)) and RRKM calculations. The overall barrierless and exoergic reaction involves indirect reaction dynamics and preferentially starts with the addition of the 1-propynyl radical with its radical center to the carbon-carbon double bond at the C1 position atom of 2-methylpropene. Initially formed C_7H_{11} intermediates either emit atomic hydrogen or undergo isomerization via [1,2-H] shift from the CH_3 or CH_2 group prior to atomic hydrogen loss preferentially leading to 1,2,4-trimethylvinylacetylene (2-methylhex-2-en-4-yne; **p1**) as the primary product. The molecular structures of the collisional complexes promote hydrogen atom loss channels. RRKM results also reveal that hydrogen elimination channels dominate, with a branching ratio exceeding 70%. The methyl group of the 1-propynyl radical reactant is not involved in the reaction mechanism and remains as a spectator throughout the reaction. Since the reaction of the 1-propynyl radical with 2-methylpropene has no entrance barrier, is exoergic, and all transition states involved are located below the energy of the separated reactants, bimolecular collisions are feasible to form trimethylsubstituted 1,3-enyne (**p1**) via a single collision event even at temperatures as low as 10 K prevailing in cold molecular clouds such as G+0.693.[34] These findings have strong

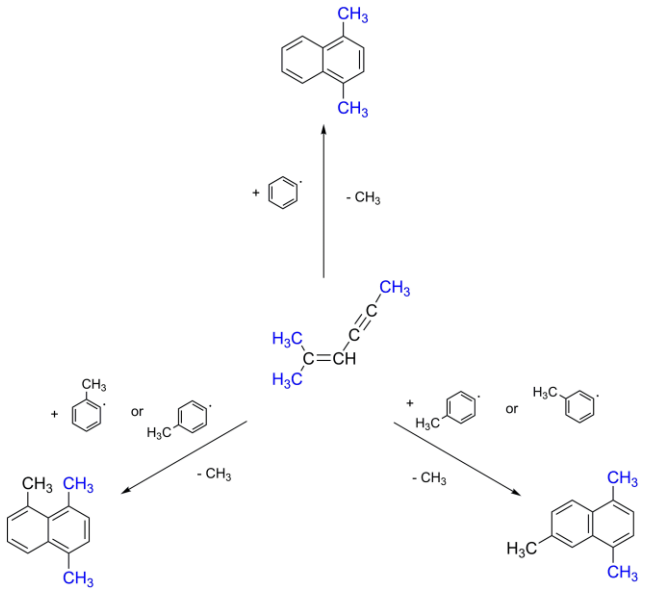

Figure 7. Reaction pathways leading to the formation of distinct methylsubstituted naphthalenes via the HAVA mechanism.

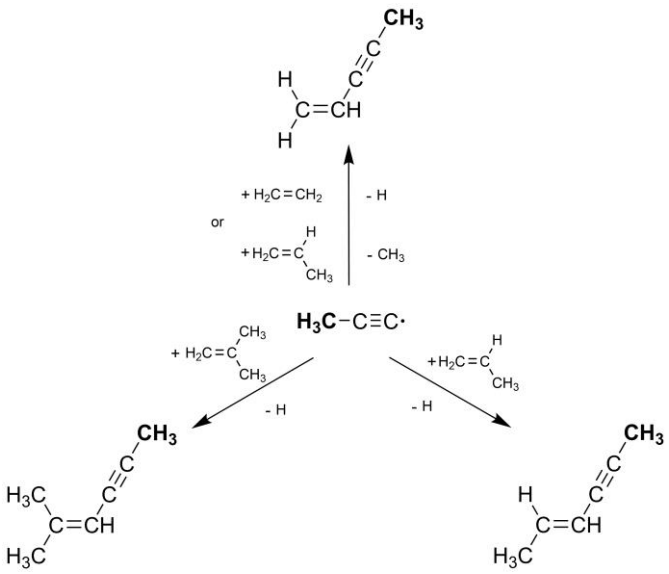

Figure 8. Bimolecular reactions of the 1-propynyl radical with substituted alkenes studied under single collision conditions.

implications for the complex hydrocarbon chemistry in cold molecular clouds. Recently, 2-methylpropene was detected in the cold molecular cloud G+0.693;[34] 1-propynyl is likely to be present in the same cold molecular clouds since its potential precursor methylacetylene holds a high fractional abundance of 1.3×10^{-8}.[55] Therefore, based on our combined experimental and computational study, 1,2,4-trimethylvinylacetylene (2-methylhex-2-en-4-yne; **p1**) is likely to be formed in G+0.693. The formation of this trimethylsubstituted vinylacetylene is a potential starting point to fundamental molecular mass growth processes leading to di- and trimethyl substituted naphthalenes upon reactions with phenyl (C_6H_5)[21] and tolyl radicals ($CH_3C_6H_5$)[23] (Fig. 7) via the barrierless HAVA mechanism. Traditionally, the HAVA ends with hydrogen loss from the R^1 or R^2 position in vinylacetylene (Fig. 2); however, in 1,2,4-trimethylvinylacetylene (2-methylhex-2-en-4-yne; **p1**), there is no hydrogen at R^1 or R^2, and the reaction can only terminate through methyl elimination. This would provide dimethyl substituted naphthalenes in the reaction of 1,2,4-trimethylvinylacetylene (2-methylhex-2-en-4-yne; **p1**) with the phenyl radical, but trimethyl substituted naphthalenes upon reaction with tolyl radicals (Fig. 7). However, it still remains to be verified whether the barrierless character of vinylacetylene addition by its terminal vinylic carbon atom to (substituted) phenyl radicals will hold with methyl substituents at R^1 or R^2 because of the steric hindrance by these bulky groups. The reaction mechanism of 1-propynyl with 2-methylpropene follows the main trends that were found for the reactions of the 1-propynyl radical with unsaturated hydrocarbons[25,45–51]: (i) the reaction starts with barrierless addition of the radical center to the unsaturated bond, (ii) the overall process is exoergic, (iii) all transition states involved are located below the energy of the separated reactants, (iv) the methyl group of the 1-propynyl radical reactant is not involved in the reaction mechanism and plays a spectator role. Overall, all reactions of the 1-propynyl radical with olefines studies in our laboratory are barrierless and yield methyl substituted 1,3-enynes as dominant products (Fig. 8).[25,45] Similar to 1,2,4-trimethylvinylacetylene (2-methylhex-2-en-4-yne; **p1**), these substituted vinylacetylenes can further engage in molecular mass growth processes via, e.g., HAVA, in cold molecular clouds.

Author Contributions

Supervision and Funding acquisition - R. I. K., A.M.M; Formal Analysis - I.A.M.; Investigation - I.A.M., Z.Y. and S. J. G. carried out the experimental measurements, A.A.N. - carried out the theoretical analysis; Writing original draft - I.A.M.; Writing – review & editing - R. I. K., A.M.M., I.A.M.

Conflicts of interest

There are no conflicts to declare.

Acknowledgements

This work was supported by the U.S. Department of Energy, Basic Energy Sciences, by grant no. DE-FG02-03ER15411 to the University of Hawaii at Manoa and by grant no. DE-FG02-04ER15570 to the Florida International University.

Notes and references

1 C. P. Endres, S. Schlemmer, P. Schilke, J. Stutzki and H. S. P. Müller, The Cologne Database for Molecular Spectroscopy, CDMS, in the Virtual Atomic and Molecular Data Centre, VAMDC, *Journal of Molecular Spectroscopy*, 2016, **327**, 95–104.

2 R. I. Kaiser and N. Hansen, An Aromatic Universe – A Physical Chemistry Perspective, *J. Phys. Chem. A*, 2021, **125**, 3826–3840.
3 L. d'Hendecourt and P. Ehrenfreund, Spectroscopic properties of polycyclic aromatic hydrocarbons (PAHs) and astrophysical implications, *Advances in Space Research*, 1997, **19**, 1023–1032.
4 E. F. van Dishoeck, Astrochemistry: From Molecular Clouds to Planetary Systems: IAU Symposium 1971, *PUBL ASTRON SOC PAC*, 2000, **112**, 286–287.
5 H. Naraoka, A. Shimoyama and K. Harada, Isotopic evidence from an Antarctic carbonaceous chondrite for two reaction pathways of extraterrestrial PAH formation, *Earth and Planetary Science Letters*, 2000, **184**, 1–7.
6 N. Balucani, O. Asvany, Y. Osamura, L. C. L. Huang, Y. T. Lee and R. I. Kaiser, Laboratory investigation on the formation of unsaturated nitriles in Titan's atmosphere, *Planetary and Space Science*, 2000, **48**, 447–462.
7 L. Becker and T. E. Bunch, Fullerenes, fulleranes and polycyclic aromatic hydrocarbons in the Allende meteorite, *Meteoritics & Planetary Science*, 1997, **32**, 479–487.
8 M. C. McCarthy and B. A. McGuire, Aromatics and Cyclic Molecules in Molecular Clouds: A New Dimension of Interstellar Organic Chemistry, *J. Phys. Chem. A*, 2021, **125**, 3231–3243.
9 A. M. Ricks, G. E. Douberly and M. A. Duncan, The infrared spectrum of protonated naphthalene and its relevance for the unidentified infrared bands, *ApJ*, 2009, **702**, 301–306.
10 J. Cernicharo, A. M. Heras, A. G. G. M. Tielens, J. R. Pardo, F. Herpin, M. Guélin and L. B. F. M. Waters, Infrared Space Observatory's Discovery of C_4H_2, C_6H_2, and Benzene in CRL 618, *ApJ*, 2001, **546**, L123.
11 J. Cernicharo, M. Agúndez, C. Cabezas, B. Tercero, N. Marcelino, J. R. Pardo and P. de Vicente, Pure hydrocarbon cycles in TMC-1: Discovery of ethynyl cyclopropenylidene, cyclopentadiene, and indene, *A&A*, 2021, **649**, L15.
12 A. M. Burkhardt, K. L. K. Lee, P. B. Changala, C. N. Shingledecker, I. R. Cooke, R. A. Loomis, H. Wei, S. B. Charnley, E. Herbst, M. C. McCarthy and B. A. McGuire, Discovery of the Pure Polycyclic Aromatic Hydrocarbon Indene (c-C_9H_8) with GOTHAM Observations of TMC-1, *ApJL*, 2021, **913**, L18.
13 B. A. McGuire, A. M. Burkhardt, S. Kalenskii, C. N. Shingledecker, A. J. Remijan, E. Herbst and M. C. McCarthy, Detection of the aromatic molecule benzonitrile (c-C_6H_5CN) in the interstellar medium, *Science*, 2018, **359**, 202–205.
14 M. L. Sita, P. B. Changala, C. Xue, A. M. Burkhardt, C. N. Shingledecker, K. L. K. Lee, R. A. Loomis, E. Momjian, M. A. Siebert, D. Gupta, E. Herbst, A. J. Remijan, M. C. McCarthy, I. R. Cooke and B. A. McGuire, Discovery of Interstellar 2-Cyanoindene (2-C_9H_7CN) in GOTHAM Observations of TMC-1, *ApJL*, 2022, **938**, L12.
15 D. Loru, C. Cabezas, J. Cernicharo, M. Schnell and A. L. Steber, Detection of ethynylbenzene in TMC-1 and the interstellar search for 1,2-diethynylbenzene, *A&A*, 2023, **677**, A166.
16 J. Cernicharo, M. Agúndez, R. I. Kaiser, C. Cabezas, B. Tercero, N. Marcelino, J. R. Pardo and P. de Vicente, Discovery of benzyne, o-C_6H_4, in TMC-1 with the QUIJOTE line survey, *A&A*, 2021, **652**, L9.
17 B. A. McGuire, R. A. Loomis, A. M. Burkhardt, K. L. K. Lee, C. N. Shingledecker, S. B. Charnley, I. R. Cooke, M. A. Cordiner, E. Herbst, S. Kalenskii, M. A. Siebert, E. R. Willis, C. Xue, A. J. Remijan and M. C. McCarthy, Detection of two interstellar polycyclic aromatic hydrocarbons via spectral matched filtering, *Science*, 2021, **371**, 1265–1269.
18 B. M. Jones, F. Zhang, R. I. Kaiser, A. Jamal, A. M. Mebel, M. A. Cordiner and S. B. Charnley, Formation of benzene in the interstellar medium, *Proc. Natl. Acad. Sci. U.S.A.*, 2011, **108**, 452–457.
19 L. Zhao, R. I. Kaiser, B. Xu, U. Ablikim, M. Ahmed, M. M. Evseev, E. K. Bashkirov, V. N. Azyazov and A. M. Mebel, Low-temperature formation of polycyclic aromatic hydrocarbons in Titan's atmosphere, *Nat Astron*, 2018, **2**, 973–979.
20 B. Shukla and M. Koshi, A novel route for PAH growth in HACA based mechanisms, *Combustion and Flame*, 2012, **159**, 3589–3596.
21 D. S. N. Parker, F. Zhang, Y. S. Kim, R. I. Kaiser, A. Landera, V. V. Kislov, A. M. Mebel and A. G. G. M. Tielens, Low temperature formation of naphthalene and its role in the synthesis of PAHs (Polycyclic Aromatic Hydrocarbons) in the interstellar medium, *Proc. Natl. Acad. Sci. U.S.A.*, 2012, **109**, 53–58.
22 T. Yang, L. Muzangwa, R. I. Kaiser, A. Jamal and K. Morokuma, A combined crossed molecular beam and theoretical investigation of the reaction of the meta-tolyl radical with vinylacetylene – toward the formation of methylnaphthalenes, *Phys. Chem. Chem. Phys.*, 2015, **17**, 21564–21575.
23 D. S. N. Parker, B. B. Dangi, R. I. Kaiser, A. Jamal, M. N. Ryazantsev, K. Morokuma, A. Korte and W. Sander, An Experimental and Theoretical Study on the Formation of 2-Methylnaphthalene ($C_{11}H_{10}$/$C_{11}H_3$ D_7) in the Reactions of the Para-Tolyl (C_7H_7) and Para-Tolyl-d7 (C_7D_7) with Vinylacetylene (C_4H_4), *J. Phys. Chem. A*, 2014, **118**, 2709–2718.
24 R. I. Kaiser, D. S. N. Parker and A. M. Mebel, Reaction Dynamics in Astrochemistry: Low-Temperature Pathways to Polycyclic Aromatic Hydrocarbons in the Interstellar Medium, *Annu. Rev. Phys. Chem.*, 2015, **66**, 43–67.
25 I. A. Medvedkov, A. A. Nikolayev, C. He, Z. Yang, A. M. Mebel and R. I. Kaiser, A combined experimental and computational study on the reaction dynamics of the 1-propynyl (CH_3CC, X^2A_1) – propylene (CH_3CHCH_2, X^1A') system: formation of 1,3-dimethylvinylacetylene ($CH_3CCCHCHCH_3$, X^1A') under single collision conditions, *Mol. Phys.*, 2023, e2234509.
26 M. Jourdain de Muizon, L. B. D'Hendecourt and T. R. Geballe, Three micron spectroscopy of IRAS sources : observed and laboratory signatures of PAHs., *Astron. Astrophys.*, 1990, **235**, 367.
27 M. Jourdain de Muizon, P. Cox and J. Lequeux, A survey of infrared features in HII regions, planetary nebulae and proto-planetary nebulae from the IRAS-LRS data base., *Astronomy and Astrophysics Supplement Series*, 1990, **83**, 337–355.
28 S. Kwok, The mystery of unidentified infrared emission bands, *Astrophys. Space Sci*, 2022, **367**, 16.
29 X. J. Yang, R. Glaser, A. Li and J. X. Zhong, The Carriers of the Interstellar Unidentified Infrared Emission Features: Constraints from the Interstellar C-H Stretching Features At 3.2-3.5 μm, *Astrophys. J.*, 2013, **776**, 110.
30 A. Li and B. T. Draine, The Carriers of the Interstellar Unidentified Infrared Emission Features: Aromatic or Aliphatic?, *Astrophys. J.*, 2012, **760**, L35.
31 B. J. Hrivnak, T. R. Geballe and S. Kwok, A Study of the 3.3 and 3.4 μm Emission Features in Proto–Planetary Nebulae, *ApJ*, 2007, **662**, 1059–1066.
32 T. R. Geballe, A. G. G. M. Tielens, S. Kwok and B. J. Hrivnak, Unusual 3 micron emission features in three proto-planetary nebulae, *Astrophys. J.*, 1992, **387**, L89.
33 S. Kwok and Y. Zhang, Mixed aromatic–aliphatic organic nanoparticles as carriers of unidentified infrared emission features, *Nature*, 2011, **479**, 80–83.
34 M. Fatima, H. S. P. Müller, O. Zingsheim, F. Lewen, V. M. Rivilla, I. Jiménez-Serra, J. Martín-Pintado and S. Schlemmer, Millimetre and submillimetre spectroscopy of isobutene and its detection in the molecular cloud G+0.693, *Astron. Astrophys.*, DOI:10.1051/0004-6361/202347112.
35 R. I. Kaiser, Experimental Investigation on the Formation of Carbon-Bearing Molecules in the Interstellar Medium via

Neutral–Neutral Reactions, *Chem. Rev.*, 2002, **102**, 1309–1358.

36 X. Gu, Y. Guo, F. Zhang, A. M. Mebel and R. I. Kaiser, Reaction dynamics of carbon-bearing radicals in circumstellar envelopes of carbon stars, *Faraday Discuss.*, 2006, **133**, 245.

37 R. I. Kaiser and A. M. Mebel, The reactivity of ground-state carbon atoms with unsaturated hydrocarbons in combustion flames and in the interstellar medium, *International Reviews in Physical Chemistry*, 2002, **21**, 307–356.

38 X. Gu and R. I. Kaiser, Reaction Dynamics of Phenyl Radicals in Extreme Environments: A Crossed Molecular Beam Study, *Acc. Chem. Res.*, 2009, **42**, 290–302.

39 A. M. Mebel and R. I. Kaiser, Formation of resonantly stabilised free radicals via the reactions of atomic carbon, dicarbon, and tricarbon with unsaturated hydrocarbons: theory and crossed molecular beams experiments, *Int. Rev. Phys. Chem.*, 2015, **34**, 461–514.

40 R. I. Kaiser and A. M. Mebel, On the formation of polyacetylenes and cyanopolyacetylenes in Titan's atmosphere and their role in astrobiology, *Chem. Soc. Rev.*, 2012, **41**, 5490.

41 X. Gu, R. I. Kaiser and A. M. Mebel, Chemistry of Energetically Activated Cumulenes—From Allene (H_2CCCH_2) to Hexapentaene ($H_2CCCCCCH_2$), *ChemPhysChem*, 2008, **9**, 350–369.

42 L. Zhao, R. I. Kaiser, W. Lu, B. Xu, M. Ahmed, A. N. Morozov, A. M. Mebel, A. H. Howlader and S. F. Wnuk, Molecular mass growth through ring expansion in polycyclic aromatic hydrocarbons via radical–radical reactions, *Nat Commun*, 2019, **10**, 3689.

43 J. Bouwman, M. Fournier, I. R. Sims, S. R. Leone and K. R. Wilson, Reaction Rate and Isomer-Specific Product Branching Ratios of C_2H + C_4H_8: 1-Butene, cis-2-Butene, trans-2-Butene, and Isobutene at 79 K, *J. Phys. Chem. A*, 2013, **117**, 5093–5105.

44 D. E. Woon and J.-Y. Park, Modeling chemical growth processes in Titan's atmosphere 2. Theoretical study of reactions between C_2H and ethene, propene, 1-butene, 2-butene, isobutene, trimethylethene, and tetramethylethene, *Icarus*, 2009, **202**, 642–655.

45 A. M. Thomas, L. Zhao, C. He, A. M. Mebel and R. I. Kaiser, A Combined Experimental and Computational Study on the Reaction Dynamics of the 1-Propynyl (CH_3CC) – Acetylene (HCCH) System and the Formation of Methyldiacetylene (CH_3CCCH), *J. Phys. Chem. A*, 2018, **122**, 6663–6672.

46 A. M. Thomas, C. He, L. Zhao, G. R. Galimova, A. M. Mebel and R. I. Kaiser, Combined Experimental and Computational Study on the Reaction Dynamics of the 1-Propynyl (CH_3CC)–1,3-Butadiene ($CH_2CHCHCH_2$) System and the Formation of Toluene under Single Collision Conditions, *J. Phys. Chem. A*, 2019, **123**, 4104–4118.

47 C. He, L. Zhao, A. M. Thomas, A. N. Morozov, A. M. Mebel and R. I. Kaiser, Elucidating the Chemical Dynamics of the Elementary Reactions of the 1-Propynyl Radical (CH_3CC; X^2A_1) with Methylacetylene (H_3CCCH; X^1A_1) and Allene (H_2CCCH_2; X^1A_1), *J. Phys. Chem. A*, 2019, **123**, 5446–5462.

48 C. He, L. Zhao, A. M. Thomas, G. R. Galimova, A. M. Mebel and R. I. Kaiser, A combined experimental and computational study on the reaction dynamics of the 1-propynyl radical (CH_3CC; X^2A_1) with ethylene (H_2CCH_2; X^1A_{1g}) and the formation of 1-penten-3-yne ($CH_2CHCCCH_3$; X^1A'), *Phys. Chem. Chem. Phys.*, 2019, **21**, 22308–22319.

49 A. M. Thomas, S. Doddipatla, R. I. Kaiser, G. R. Galimova and A. M. Mebel, A Barrierless Pathway Accessing the C_9H_9 and C_9H_8 Potential Energy Surfaces via the Elementary Reaction of Benzene with 1-Propynyl, *Sci. Rep.*, 2019, **9**, 17595.

50 S. Doddipatla, G. R. Galimova, H. Wei, A. M. Thomas, C. He, Z. Yang, A. N. Morozov, C. N. Shingledecker, A. M. Mebel and R. I. Kaiser, Low-temperature gas-phase formation of indene in the interstellar medium, *Sci. Adv.*, 2021, **7**, eabd4044.

51 B. B. Kirk, J. D. Savee, A. J. Trevitt, D. L. Osborn and K. R. Wilson, Molecular weight growth in Titan's atmosphere: branching pathways for the reaction of 1-propynyl radical (H_3CCC) with small alkenes and alkynes, *Phys. Chem. Chem. Phys.*, 2015, **17**, 20754–20764.

52 A. M. Burkhardt, K. Long Kelvin Lee, P. Bryan Changala, C. N. Shingledecker, I. R. Cooke, R. A. Loomis, H. Wei, S. B. Charnley, E. Herbst, M. C. McCarthy and B. A. McGuire, Discovery of the Pure Polycyclic Aromatic Hydrocarbon Indene (c-C_9H_8) with GOTHAM Observations of TMC-1, *ApJL*, 2021, **913**, L18.

53 V. V. Guzmán, J. Pety, P. Gratier, J. R. Goicoechea, M. Gerin, E. Roueff, F. Le Petit and J. Le Bourlot, Chemical complexity in the Horsehead photodissociation region, *Faraday Discuss.*, 2014, **168**, 103–127.

54 P. Gratier, L. Majumdar, M. Ohishi, E. Roueff, J. C. Loison, K. M. Hickson and V. Wakelam, A New Reference Chemical Composition for TMC-1, *Astrophys. J., Supp. Ser.*, 2016, **225**, 25.

55 L. Bizzocchi, D. Prudenzano, V. M. Rivilla, A. Pietropolli-Charmet, B. M. Giuliano, P. Caselli, J. Martín-Pintado, I. Jiménez-Serra, S. Martín, M. A. Requena-Torres, F. Rico-Villas, S. Zeng and J.-C. Guillemin, Propargylimine in the laboratory and in space: millimetre-wave spectroscopy and its first detection in the ISM,*Astron. Astrophys.*, 2020, **640**, A98.

56 I. H. Goldberg, Mechanism of neocarzinostatin action: role of DNA microstructure in determination of chemistry of bistranded oxidative damage, *Acc. Chem. Res.*, 1991, **24**, 191–198.

57 Y. Liu, M. Nishiura, Y. Wang and Z. Hou, π-Conjugated Aromatic Enynes as a Single-Emitting Component for White Electroluminescence, *J. Am. Chem. Soc.*, 2006, **128**, 5592–5593.

58 G. Chen, L. Wang, D. W. Thompson and Y. Zhao, Highly π-Extended TTF Analogues with a Conjugated Macrocyclic Enyne Core, *Org. Lett.*, 2008, **10**, 657–660.

59 X. Bao, J. Ren, Y. Yang, X. Ye, B. Wang and H. Wang, 2-Activated 1,3-enynes in enantioselective synthesis, *Org. Biomol. Chem.*, 2020, **18**, 7977–7986.

60 F. Liu, D. Qian, L. Li, X. Zhao and J. Zhang, Diastereo- and Enantioselective Gold(I)-Catalyzed Intermolecular Tandem Cyclization/[3+3]Cycloadditions of 2-(1-Alkynyl)-2-alken-1-ones with Nitrones, *Angew Chem Int Ed*, 2010, **49**, 6669–6672.

61 Y. Liu, P. Luo, Y. Fu, T. Hao, X. Liu, Q. Ding and Y. Peng, Recent advances in the tandem annulation of 1,3-enynes to functionalized pyridine and pyrrole derivatives, *Beilstein J. Org. Chem.*, 2021, **17**, 2462–2476.

62 C. Pfeffer, N. Wannenmacher, W. Frey and R. Peters, Stereo- and Regioselective Dimerization of Alkynes to Enynes by Bimetallic Syn-Carbopalladation, *ACS Catal.*, 2021, **11**, 5496–5505.

63 B. M. Trost and J. T. Masters, Transition metal-catalyzed couplings of alkynes to 1,3-enynes: modern methods and synthetic applications, *Chem. Soc. Rev.*, 2016, **45**, 2212–2238.

64 Z. Wang, C. Zhang, J. Wu, B. Li, A. Chrostowska, P. Karamanis and S.-Y. Liu, trans-Hydroalkynylation of Internal 1,3-Enynes Enabled by Cooperative Catalysis, *J. Am. Chem. Soc.*, 2023, **145**, 5624–5630.

65 M. Dörfler, N. Tschammer, K. Hamperl, H. Hübner and P. Gmeiner, Novel D3 Selective Dopaminergics Incorporating Enyne Units as Nonaromatic Catechol Bioisosteres: Synthesis, Bioactivity, and Mutagenesis Studies, *J. Med. Chem.*, 2008, **51**, 6829–6838.

66 R. I. Kaiser, P. Maksyutenko, C. Ennis, F. Zhang, X. Gu, S. P. Krishtal, A. M. Mebel, O. Kostko and M. Ahmed, Untangling the chemical evolution of Titan's atmosphere and surface–

from homogeneous to heterogeneous chemistry, *Faraday Discuss.*, 2010, **147**, 429–478.
67 Y. Guo, X. Gu, E. Kawamura and R. I. Kaiser, Design of a modular and versatile interlock system for ultrahigh vacuum machines: A crossed molecular beam setup as a case study, *Review of Scientific Instruments*, 2006, **77**, 034701.
68 N. R. Daly, Scintillation Type Mass Spectrometer Ion Detector, *Review of Scientific Instruments*, 1960, **31**, 264–267.
69 M. F. Vernon, Ph.D. Dissertation, University of California, 1983.
70 P. S. Weiss, Ph.D. Dissertation, University of California, 1986.
71 J.-D. Chai and M. Head-Gordon, Long-range corrected hybrid density functionals with damped atom–atom dispersion corrections, *Phys. Chem. Chem. Phys.*, 2008, **10**, 6615–6620.
72 T. B. Adler, G. Knizia and H.-J. Werner, A simple and efficient CCSD(T)-F12 approximation, *The Journal of Chemical Physics*, 2007, **127**, 221106.
73 G. Knizia, T. B. Adler and H.-J. Werner, Simplified CCSD(T)-F12 methods: Theory and benchmarks, *The Journal of Chemical Physics*, 2009, **130**, 054104.
74 T. H. Dunning Jr., Gaussian basis sets for use in correlated molecular calculations. I. The atoms boron through neon and hydrogen, *The Journal of Chemical Physics*, 1989, **90**, 1007–1023.
75 J. Zhang and E. F. Valeev, Prediction of Reaction Barriers and Thermochemical Properties with Explicitly Correlated Coupled-Cluster Methods: A Basis Set Assessment, *J. Chem. Theory Comput.*, 2012, **8**, 3175–3186.
76 M. J. Frisch, G. W. Trucks, H. B. Schlegel, G. E. Scuseria, M. A. Robb, J. R. Cheeseman, G. Scalmani, V. Barone, B. Mennucci, G. A. Petersson, H. Nakatsuji, M. Caricato, X. Li, H. P. Hratchian, A. F. Izmaylov, J. Bloino, G. Zheng, J. L. Sonnenberg, M. Hada, M. Ehara, K. Toyota, R. Fukuda, J. Hasegawa, M. Ishida, T. Nakajima, Y. Honda, O. Kitao, H. Nakai, T. Vreven, J. A. Montgomery, J. E. Peralta, F. Ogliaro, M. Bearpark, J. J. Heyd, E. Brothers, K. N. Kudin, V. N. Staroverov, R. Kobayashi, J. Normand, K. Raghavachari, A. Rendell, J. C. Burant, S. S. Iyengar, J. Tomasi, M. Cossi, N. Rega, J. M. Millam, M. Klene, J. E. Knox, J. B. Cross, V. Bakken, C. Adamo, J. Jaramillo, R. Gomperts, R. E. Stratmann, O. Yazyev, A. J. Austin, R. Cammi, C. Pomelli, J. W. Ochterski, R. L. Martin, K. Morokuma, V. G. Zakrzewski, G. A. Voth, P. Salvador, J. J. Dannenberg, S. Dapprich, A. D. Daniels, Ö. Farkas, J. B. Foresman, J. V. Ortiz, J. Cioslowski and D. J. Fox, *Gaussian* 09, Revision D.1, Gaussian., Gaussian Inc.: Wallingford, CT, 2009.
77 H.-J. Werner, P. J. Knowles, R. Lindh, F. R. Manby, M. Schütz, P. Celani, T. Korona, G. Rauhut, R. D. Amos and A. Bernhardsson, *MOLPRO, Version 2015.1, A Package of Ab Initio Programs*, University of Cardiff: Cardiff: UK, 2015.
78 J. I. Steinfeld, J. S. Francisco and W. L. Hase, *Chemical Kinetics and Dynamics*, Pearson, Upper Saddle River, N.J, 2nd edition., 1998.
79 R. D. Levine, *Molecular reaction dynamics*, Cambridge University Press, Cambridge, UK, 2005.